ISA
TRANSACTIONS®

ISA Transactions 43 (2004) 343–359

Embedded estimator in predictive feedback control

Leonardo L. Giovanini*

Industrial Control Centre, University of Strathclyde, Graham Hills Building, 50 George Street, Glasgow G1 1QE, Scotland

(Received 15 April 2003; accepted 28 September 2003)

Abstract

In this work, a new approach to design predictive feedback control for SISO systems is presented. The proposed formulation relies on the development of a single step predictor based on an autoregressive moving average with external input (ARMAX) model. Although no explicit observer is actually involved in the implementation, this predictor implicitly includes one since the input-output model subsumes an observer. Exploiting this idea the resulting ARMAX model is extended to include extra outputs to improve the quality of the prediction for systems with large time delay and nonmeasurable disturbances. The resulting predictor is used to develop a predictive feedback controller. This new formulation of predictive feedback control includes feedback and feedforward actions. Simulations of two linear systems illustrate the applicability of the control algorithm. © 2004 ISA—The Instrumentation, Systems, and Automation Society.

Keywords: Predictive control; Dynamic observers; Inferential control; Feedback/Feedforward control

1. Introduction

In the well-known state-space model, the relationship between the input and output variables is described in terms of an intermediate quantity called the state vector. On the other hand, a typical input-output model describes the current output as a linear combination of past input and output measurements. One such model is the autoregressive moving average with external input (ARMAX), which is the most commonly used model in discrete control.

Many control techniques have been developed for state-space and ARMAX models. One of the most relevant is the model predictive control (MPC) techniques. The predictive control concepts can be thought of as an extension of the one-step ahead approach of l_2 optimal control theory, which calls for an approximate one-step ahead inversion of the input-output model to produce the control action. This simple inversion approach is not suitable for a nonminimum phase system, which will cause the control input to grow unbounded while the controlled output remain bounded. This problem can be overcome by introducing a proper dynamic into the controller structure [1,2] or varying the time index of the output that is controlled [2–4].

To understand the connection between the state-space and input-output model-based control approaches, it is important to understand how an input-output model relates to the space-state model and vice versa. It is well known that starting with an input-output model, such as an ARMAX model, one can convert it to a controllable and/or observable canonical space-state form. The reverse connection from a space-state model to an equivalent ARMAX model can also be carried out via canonical forms too. Motivated

*Tel: +44-141-548 2666; fax: +44-141-552 2487.
E-mail address: leonardo.giovanini@eee.strath.ac.uk

by these results of realization theory, we look for predictors that can make use of implicit observer information embedded in an input-output model. We exploit this understanding in the relationship between the space-state and ARMAX model to derive a single-step predictor capable of retaining the key benefits of the space-state approach to improve the accuracy of the prediction. The resulting predictor is employed to build a predictive feedback controller that includes feedback and feedforward actions.

The organization of the paper is as follow: in Section 2, the expressions for a general J-step ahead output prediction are presented. The relationship between the coefficients of the single-step predictor and the coefficients of ARMAX model is established. In Section 3 the relationship between the space-state and ARMAX models is analyzed. The relationship between the space-state matrices and the coefficients of the equivalent ARMAX model is explained in terms of an observer matrix, whose dynamic behavior defines the order of the model. Then, exploiting this idea the resulting ARMAX model is extended to include additional system outputs to improve the prediction for systems with time delay and nonmeasurable disturbances. In Section 4 the basic formulation for the single-prediction controller design is derived and stability analysis is carried out. A simple criterion for choosing the prediction time is derived. It guarantees the robust stability of the closed-loop system. In Section 5 a direct feedback mode is introduced in order to improve the overall system performance. The stability of the resulting structure is analyzed. The main result is the independent selection of each element of the predictive feedback controller. In Section 6 we show the results obtained from the application of the proposed algorithm to two linear systems. Finally, the conclusions are presented in Section 7.

2. Single-step output predictor

Consider the SISO system depicted in Fig. 1, where q^{-1} is the backward shift operator, $d_m(k)$ is the load disturbance, and $d(k)$ is the nonmeasurable disturbance. In the following we assume that a model of $G_d(q^{-1})$ is available and $d_m(k)$ is a measurable deterministic disturbance. The process may also be subject to many disturbances. They can be collectively represented by

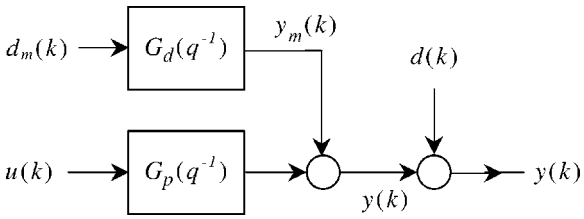

Fig. 1. Process model and disturbance.

one nonmeasurable disturbance $d(k)$ entering the process at the output. Employing the models of the system $\tilde{G}_p(q^{-1})$ and $\tilde{G}_d(q^{-1})$, the output at time k is described by the difference equation

$$\tilde{y}(k) = -\sum_{j=1}^{n_y} \tilde{a}_i y(k-j) + \sum_{j=0}^{n_u} \tilde{b}_j u(k-t_d-j) + \sum_{j=0}^{n_d} \tilde{c}_j d_m(k-j) + \tilde{d}(k), \quad n_y \geqslant n_u, n_y \geqslant n_d, \tag{1}$$

which is also referred to in the literature as the ARMAX model. In this case, the nonmeasurable disturbance $\tilde{d}(k)$ lumps together the unmeasured disturbance $d(k)$ and inaccuracies due to plant-model mismatch

$$\tilde{d}(k) = (G_p(q^{-1}) - \tilde{G}_p(q^{-1}))u(k) + d(k).$$

Defining the following variables

$$p \geqslant \max(n_y, n_u + t_d, n_d), \tag{2}$$

$$\tilde{\alpha}_j = \begin{cases} -\tilde{a}_j, & j = 1,2,\ldots,n_y, \\ 0, & j > n_y, \end{cases}$$

$$\tilde{\beta}_j = \begin{cases} 0, & j = 1,2,\ldots,t_d, \\ \tilde{b}_j, & j = t_d+1,\ldots,t_d+n_u, \\ 0, & j > t_d+n_u, \end{cases}$$

$$\tilde{\gamma}_j = \begin{cases} \tilde{c}_j, & j = 0,1,2,\ldots,n_d, \\ 0, & j > n_d, \end{cases} \tag{3}$$

we can write the system output $\tilde{y}(k)$ as follows:

$$\tilde{y}(k) = \sum_{j=1}^{p} \tilde{\alpha}_j y(k-j) + \sum_{j=0}^{p} \tilde{\beta}_j u(k-j) + \sum_{j=0}^{p} \tilde{\gamma}_j d_m(k-j) + \tilde{d}(k). \tag{4}$$

By shifting a time step, obtain the one-step ahead prediction:

$$\hat{y}(1,k)=\tilde{\alpha}_1\hat{y}(k)+\sum_{j=1}^{p-1}\tilde{\alpha}_{j+1}y(k-j)+\tilde{\beta}_0u(k+1)+\sum_{j=1}^{p}\tilde{\beta}_ju(k+1-j)+\tilde{\gamma}_0d_m(k+1)+\sum_{j=1}^{p}\tilde{\gamma}_jd_m(k+1-j)+\tilde{d}(k+1), \quad (5)$$

where the first index stands for the number of step ahead samples for which the system output is computed $(k+1)$ and the second one is the time when the prediction is computed (k). Replacing $\tilde{y}(k)$ from Eqs. (4) into (5) yields

$$\hat{y}(1,k)=\sum_{j=1}^{p-1}\tilde{\alpha}_j^1y(k-j)+\tilde{\beta}_0u(k+1)+\sum_{j=1}^{p}\tilde{\beta}_j^1u(k+1-j)+\tilde{\gamma}_0d_m(k+1)+\sum_{j=1}^{p}\tilde{\gamma}_j^1d_m(k+1-j)+\tilde{d}(k+1), \quad (6)$$

where the coefficients of the *predictor* are given by

$$\begin{aligned}\tilde{\alpha}_j^1&=\tilde{\alpha}_{j+1}+\tilde{\alpha}_1\tilde{\alpha}_j, \quad j=1,2,\ldots,p-1,\\ \tilde{\beta}_j^1&=\tilde{\beta}_{j+1}+\tilde{\alpha}_1\tilde{\beta}_j,\\ \tilde{\gamma}_j^1&=\tilde{\gamma}_{j+1}+\tilde{\alpha}_1\tilde{\gamma}_j,\\ \tilde{\alpha}_p^1&=\tilde{\alpha}_1\tilde{\alpha}_p,\\ \tilde{\beta}_p^1&=\tilde{\alpha}_1\tilde{\beta}_p,\\ \tilde{\gamma}_p^1&=\tilde{\alpha}_1\tilde{\gamma}_p.\end{aligned} \quad (7)$$

The system output at time $k+1$, in the absence of the output measurement at time k, can be expressed as a linear combination of past input and output data. In this notation, the current output $\tilde{y}(k)$ is given by $\hat{y}(0,k)$ with the coefficients given by $\tilde{\alpha}_j^0=\tilde{\alpha}_j$ and $\tilde{\beta}_j^0=\tilde{\beta}_j$, $j=0,1,2,\ldots,p$.

Applying the same procedure J times the system output may be expressed at time $k+J$ through

$$\hat{y}(J,k)=\sum_{j=0}^{J}\tilde{\beta}_0^{J-j}u(k+j)+\sum_{j=1}^{p}\tilde{\alpha}_j^Jy(k-j)+\sum_{j=1}^{p}\tilde{\beta}_j^Ju(k-j)+\sum_{j=0}^{J}\tilde{\gamma}_0^{J-j}d_m(k+j)+\sum_{j=1}^{p}\tilde{\gamma}_j^Jd_m(k-j)+\tilde{d}(k+J), \quad (8)$$

where the coefficients $\tilde{\alpha}_j^J,\tilde{\beta}_j^J$ and $\tilde{\gamma}_j^J$ are given by

$$\tilde{\alpha}_j^J=\tilde{\alpha}_{j+1}+\sum_{l=1}^{J}\tilde{\alpha}_l\tilde{\alpha}_j^{J-l}, \quad J\leqslant p, \quad j=0,1,\ldots,p,$$

$$\tilde{\beta}_j^J=\tilde{\beta}_{j+1}+\sum_{l=1}^{J}\tilde{\alpha}_l\tilde{\beta}_j^{J-l}, \quad (9a)$$

$$\tilde{\gamma}_j^J=\tilde{\gamma}_{j+1}+\sum_{l=1}^{J}\tilde{\alpha}_l\tilde{\gamma}_j^{J-l},$$

$$\tilde{\alpha}_j^J=\sum_{l=1}^{p}\tilde{\alpha}_l\tilde{\alpha}_j^{J-l}, \quad J>p,$$

$$\tilde{\beta}_j^J=\sum_{l=1}^{p}\tilde{\alpha}_l\tilde{\beta}_j^{J-l}, \quad (9b)$$

$$\tilde{\gamma}_j^J=\sum_{l=1}^{p}\tilde{\alpha}_l\tilde{\gamma}_j^{J-l}.$$

Equation (8) defines a *J-step ahead prediction*, it shows the effect of all inputs, past and future, on the output. Observation of Eq. (9b) shows that $\tilde{\alpha}_j^J$, $\tilde{\beta}_j^J$ and $\tilde{\gamma}_j^J$ $\forall J>p$ are a linear combination of its past p parameters weighted by the parameters $\tilde{\alpha}_l$ $l=1,2,\ldots,p$.

*Lemma 1: The coefficients $\tilde{\beta}_0^j$ and $\tilde{\gamma}_0^j$ are the j*th *of the impulse response coefficients of $\tilde{G}_p$ and $\tilde{G}_d$, respectively.*

Proof: See Appendix A.

Lemma 2: The coefficients $\tilde{\alpha}_l$ $l=1,2,\ldots,p$ represent the observer gains that are used to compute an observer for state estimation.

Proof: See Goodwin and Sin [5].

Employing the backward shift operator q^{-1} define the quantities

$$\tilde{P}_y^y(J,q^{-1})=\sum_{j=1}^{p}\tilde{\alpha}_j^J q^{-j},$$

$$\tilde{P}_u^y(J,q^{-1})=\sum_{j=1}^{p}\tilde{\beta}_j^J q^{-j}, \tag{10}$$

$$\tilde{P}_d^m(J,q^{-1})=\sum_{j=1}^{p}\tilde{\gamma}_j^J q^{-j},$$

then the prediction (8) can be written as the following:

$$\hat{y}(J,k)=\sum_{j=0}^{J}\tilde{h}_{J-j}u(k+j)+\tilde{P}_u^y(J,q^{-1})u(k)+\tilde{P}_y^y(J,q^{-1})y(k)+\sum_{j=0}^{J}\tilde{h}_{J-j}^m u(k+j)+\tilde{P}_d^m(J,q^{-1})d_m(k)+\tilde{d}(k+J), \tag{11}$$

where $\tilde{h}_j$ and $\tilde{h}_j^m$ are the jth coefficients of the impulse responses of $\tilde{G}_p$ and $\tilde{G}_d$, respectively. Since future control actions are unknown, this prediction is not realizable. To turn it realizable a statement must be made about how the input variables are going to move in the future. For example, the simplest rule is to assume that all the inputs will not move in future,

$$u(k+j)=u(k+j-1),\quad \forall j=0,1,\ldots,J,$$
$$d_m(k+j+1)=d_m(k+j), \tag{12}$$
$$\tilde{d}(k+j+1)=\tilde{d}(k+j),$$

which implies that the future changes are equal to zero. Then, the prediction (11) becomes

$$\hat{y}^0(J,k)=\tilde{a}_J u(k-1)+\tilde{P}_u^y(J,q^{-1})u(k)+\tilde{P}_y^y(J,q^{-1})y(k)+\tilde{a}_J^m d_m(k)+\tilde{P}_d^m(J,q^{-1})d_m(k)+\tilde{d}(k), \tag{13}$$

where $\tilde{a}_J$ and $\tilde{a}_J^m$ are the Jth coefficients of step responses of $\tilde{G}_p$ and $\tilde{G}_d$, respectively, and the superscript zero recalls the conditions (12) are included.

The disturbance term $\tilde{d}(k)$ is computed from the output measurement $y(k)$ and the system model through

$$\tilde{d}(k)=y(k)-\hat{y}(0,k),$$

this term lumps together possible unmeasured disturbance and inaccuracies due to plant-model mismatch. Replacing this term in Eq. (13) and rearranging we obtain the *corrected open-loop prediction* given by

$$\hat{y}^0(J,k)=[1+\mathcal{P}_y^y(J,q^{-1})]y(k)+[\tilde{a}_J q^{-1}+\mathcal{P}_u^y(J,q^{-1})]u(k)+[\tilde{a}_J^m+\mathcal{P}_d^m(J,q^{-1})]d_m(k), \tag{14}$$

where

$$\mathcal{P}_y^y(J,q^{-1})=\tilde{P}_y^y(J,q^{-1})-\tilde{P}_y^y(0,q^{-1}), \tag{15a}$$

$$\mathcal{P}_u^y(J,q^{-1})=\tilde{P}_u^y(J,q^{-1})-\tilde{P}_u^y(0,q^{-1}), \tag{15b}$$

$$\mathcal{P}_d^m(J,q^{-1})=\tilde{P}_d^m(J,q^{-1})-\tilde{P}_d^m(0,q^{-1}). \tag{15c}$$

The restriction of the measurability of the load disturbance $d_m(k)$, assumed to develop the corrected prediction can be removed if the system has analytic redundancy. In this case we can build an ARMAX that provides an estimation of the disturbance. In Section 3 we will show how to build this model, but first we will analyze the relationship between the space-state and ARMAX models. The relationship between the space-state matrices and the coefficients of the equivalent ARMAX model is explained in terms of an observer matrix, which depends on the observer gain that determines the dynamics of the observer and the order of the ARMAX model. Exploiting this idea and using all the information available in the outputs, the resulting ARMAX model is extended to estimate the nonmeasurable disturbance from the input and outputs of the system.

3. Implicit observer in ARX model

To analyze the relationship between ARMAX and space-state models, let us consider the space-state model of system (4) without disturbances whose states $x(k)$ are not measurable,

$$x(k+1)=Ax(k)+Bu(k),\quad x(0)=x_0,$$
$$y(k)=Cx(k)+Du(k). \tag{16}$$

If A is stable and (A,C) is an observable pair, the system's states can be estimates through a dynamic observer,

$$\begin{aligned}\hat{x}(k+1)&=(A-KC)\hat{x}(k)+(B-KD)u(k)\\&\quad+Ky(k),\quad \hat{x}(0)=\hat{x}_0,\\\hat{y}(0,k)&=C\hat{x}(k)+Du(k),\end{aligned}\tag{17}$$

where K is the observer gain that is computed using the Riccatti equation with the covariance matrix equal to zero [6]. In case of a stochastic system the covariance matrix is nonzero, and the observer (17) becomes the Kalman filter. Defining the dynamic filter and gain matrices,

$$\mathcal{A}=A-KC,\tag{18a}$$

$$\mathcal{B}=B-KD,\tag{18b}$$

the filter (17) can be expressed in the following form:

$$\hat{x}(k+1)=\mathcal{A}\hat{x}(k)+\mathcal{B}u(k)+Ky(k),$$

$$\hat{y}(0,k)=C\hat{x}(k)+Du(k).$$

Propagating this equation forward in time k times, starting from $k=0$, one obtains the system output at time k,

$$\hat{y}(0,k)=C\mathcal{A}^k\hat{x}(0)+\sum_{i=1}^{k}C\mathcal{A}^{i-1}\mathcal{B}u(k-i)+\sum_{i=1}^{k}C\mathcal{A}^{i-1}Ky(k-i)+Du(k).$$

Observe that the current output not only depends on the initial state, but also on the last k control actions and system output. The contribution of the states depends on the dynamic of the filter, so if k is large enough to dismiss the contribution of the initial state $\hat{x}(0)$ to the prediction

$$\mathcal{A}^k=(A-KC)^k\approx 0,\quad k>p,\tag{19}$$

what is equivalent to the dynamics of the filter has vanished some steps ago, the system output can be approximated through

$$\hat{y}(0,k)=\sum_{i=1}^{p}C\mathcal{A}^{i-1}\mathcal{B}u(k-i)+\sum_{i=1}^{p}C\mathcal{A}^{i-1}Ky(k-i)+Du(k).\tag{20}$$

Note that this result is independent of the actual system dynamics, which may still be in the transient portion after p time steps. The last equation is exactly the same as the ARMAX model (4) without disturbances. Besides, comparing Eqs. (4) and (20) reveals that the coefficients $\tilde{\alpha}_i$ and $\tilde{\beta}_i$ of ARX model are related to those of the space-state model by the following relationship:

$$\begin{aligned}\tilde{\alpha}_j&=C\mathcal{A}^{j-1}K,\quad j=1,2,\ldots,p,\\\tilde{\beta}_j&=C\mathcal{A}^{j-1}\mathcal{B},\\\tilde{\beta}_0&=D.\end{aligned}\tag{21}$$

Inspection of these equations shows that the relationship between the space-state matrices and the coefficients of the equivalent ARMAX model is given in terms of a dynamic observer matrix $\mathcal{A}$, which depends on the observer gain K [Eq. 18(a)]. This gain not only defines the dynamic of the estimator but also determines the order of ARMAX model. It is now clear that an ARMAX model of order p subsumes a deadbeat observer of order p.

3.1. Estimating the nonmeasurable disturbance

If the controlled system has analytic redundancy an estimator that is able to estimate the disturbances present in the system can be developed [7,8]. So, the ARMAX model developed from this estimator will be able to estimate the unmeasurable disturbance $\tilde{d}(k)$. For example, employing the filter proposed by Keller [9]

$$\begin{aligned}\hat{x}(k+1)&=(A-AB_d\Pi C-K\Sigma C)\hat{x}(k)+Bu(k)\\&\quad+(K\Sigma+AB_d\Pi)y(k),\\\hat{y}(0,k)&=C\hat{x}(k),\\\hat{d}(0,k)&=\Pi[y(k)-C\hat{x}(k)],\end{aligned}\tag{22}$$

where $\hat{d}(0,k)$ is the estimation of unmeasurable disturbances, B_d is the disturbance distribution matrix, and the matrices Σ and Π satisfy the isolation conditions [8]

$$\begin{aligned}\Pi CB_d&=I,\\\Sigma CB_d&=\mathbf{0}.\end{aligned}\tag{23}$$

These design conditions are required to obtain an unbiased estimation [9].

Following the procedure described in the previous section we obtain the following estimators:

$$\hat{y}(0,k)=\sum_{j=1}^{p}\mathcal{C}_y\mathcal{A}^{j-1}Bu(k-j)+\sum_{j=1}^{p}\mathcal{C}_y\mathcal{A}^{j-1}\mathcal{K}y(k-j), \quad (24a)$$

$$\hat{d}(0,k)=\Pi y(k)-\sum_{j=1}^{p}\mathcal{C}_d\mathcal{A}^{j-1}Bu(k-j)-\sum_{j=1}^{p}\mathcal{C}_d\mathcal{A}^{j-1}\mathcal{K}y(k-j), \quad (24b)$$

where the matrices $\mathcal{A}$, $\mathcal{C}_y$, $\mathcal{C}_d$, and $\mathcal{K}$ are given by

$$\begin{aligned}\mathcal{A}&=A-\mathcal{K}C,\\ \mathcal{C}_y&=C,\\ \mathcal{C}_d&=\Pi C,\\ \mathcal{K}&=K\Sigma+AB_d\Pi.\end{aligned} \quad (25)$$

From these equations it is easy to see that the parameters of the output estimator,

$$\hat{y}(0,k)=\sum_{j=1}^{p}\tilde{\beta}_{jy}u(k-j)+\sum_{j=1}^{p}\tilde{\alpha}_{jy}y(k-j), \quad (26)$$

are given by

$$\begin{aligned}\tilde{\alpha}_{jy}&=\mathcal{C}_y\mathcal{A}^{j-1}\mathcal{K}, \quad j=1,2,\ldots,p,\\ \tilde{\beta}_{jy}&=\mathcal{C}_y\mathcal{A}^{j-1}B,\end{aligned} \quad (27)$$

and the parameters of the disturbance estimator,

$$\hat{d}(0,k)=\sum_{j=1}^{p}\tilde{\beta}_{jd}u(k-j)+\sum_{j=0}^{p}\tilde{\alpha}_{jd}y(k-j), \quad (28)$$

are given by

$$\begin{aligned}\tilde{\alpha}_{0d}&=\Pi,\\ \tilde{\alpha}_{jd}&=-\mathcal{C}_d\mathcal{A}^{j-1}\mathcal{K}, \quad j=1,2,\ldots,p,\\ \tilde{\beta}_{jd}&=-\mathcal{C}_d\mathcal{A}^{j-1}B.\end{aligned} \quad (29)$$

It is important to note that both estimators use all the information available at the output of the system. So, the coefficients $\tilde{\alpha}_{jl}$ $l=y,d$ of these estimators are vectors in spite of the SISO nature of the propose scheme.

Since we have an estimate of the nonmeasurable disturbance $\tilde{d}(k)$ and its model, a better estimate of $\tilde{d}(k+J)$ can be obtained by computing its open-loop prediction $[d^0(J,k)]$. It is obtained using Eqs. (14), (15a), and (15b),

$$d^0(J,k)=[\tilde{a}_J^d q^{-1}+\mathcal{P}_u^d(J,q^{-1})]u(k)+\mathcal{P}_y^d(J,q^{-1})y(k), \quad (30)$$

with parameters of the predictors $\mathcal{P}_u^d$ and $\mathcal{P}_u^d$ given by Eqs. (25), (27), and (29).

Finally, the corrected open-loop prediction is obtained by adding Eq. (30) to Eq. (14), the result is

$$\hat{y}^0(J,k)=[1+\mathcal{P}_y(J,q^{-1})+]y(k)+[\tilde{a}_J q^{-1}+\mathcal{P}_u(J,q^{-1})]u(k)+[\tilde{a}_J^m+\mathcal{P}_d^m(J,q^{-1})]d_m(k), \quad (31)$$

where

$$\begin{aligned}\mathcal{P}_y(J,q^{-1})&=\mathcal{P}_y^y(J,q^{-1})+\mathcal{P}_y^d(J,q^{-1}),\\ \mathcal{P}_u(J,q^{-1})&=\mathcal{P}_u^y(J,q^{-1})+\mathcal{P}_u^d(J,q^{-1}),\\ \tilde{a}_J&=\tilde{a}_J^y+\tilde{a}_J^d.\end{aligned} \quad (32)$$

This predictor is the best that can be built, because it employs all the information available in the system. The controllers developed from this predictor can take faster corrective action than a standard control structure since it includes an approximate feedforward action, even if the disturbances are not measurable.

4. Single-prediction control

4.1. The control algorithm

Although the idea of using only one prediction of the system output for controlling the system is not new [2,3,10] none of these authors used the prediction time J as tuning parameter. This is the case of *single-prediction controller* [4], whose derivation procedure is quite straightforward from the open-loop prediction. Revising the assumption used to go from Eq. (11) to Eq. (13) observe that if just the only one control movement—we compute

the control change $\Delta u(k)$ in order to introduce an integral action that guarantees free offset responses—($\Delta u(k)$) is computed, then

$$\hat{y}(J,k)=\hat{y}^0(J,k)+\tilde{a}_J\Delta u(k). \tag{33}$$

Substracting this prediction from the reference variable $r(k+J)$ we obtain the predicted error

$$\hat{e}(J,k)=r(k+J)-\hat{y}(J,k). \tag{34}$$

The control action can be computed in a similar way to standard predictive controllers, by minimizing the following performance measure:

$$L(k)=\hat{e}^2(J,k)+\rho\Delta u^2(k), \quad \rho\geqslant 0. \tag{35}$$

Then, the control action that minimizes this performance index is given by

$$\Delta u(k)=K_J^{-1}\hat{e}^0(J,k), \tag{36}$$

where $\hat{e}^0(J,k)=r(k+J)-\hat{y}^0(J,k)$ and $K_J=\tilde{a}_J+\rho\tilde{a}_J^{-1}$. Giovanini [4] established the relationship between J and ρ with the closed-loop response characteristic. He found that the prediction time J is the *closed-loop settling time* for an error $\alpha|e(k_0)|$ and the control weight ρ is related to α through

$$\rho=\frac{\alpha}{1-\alpha}\tilde{a}_J^2, \quad \alpha\geqslant 0.$$

For particular choice of $\rho=0$ (what is equivalent $\alpha=0$), the performance measure (35) and the predicted closed-loop error $\hat{e}(J,k)$ become zero and the control change is given by

$$\Delta u(k)=\tilde{a}_J^{-1}\hat{e}^0(J,k). \tag{37}$$

In the following it will be assumed that $\rho=0$ to simplify the exposition. However the results that will be obtained are the same whether the control weight ρ is set to zero or not.

Using $\mathcal{Z}$ transform on Eq. (36) shows that the single-predictive control algorithm is basically an integral action applied on the predicted error

$$u(z)=\frac{1}{1-z^{-1}}\tilde{a}_J^{-1}\hat{e}^0(J,z). \tag{38}$$

Combining Eqs. (14), (34), and (38) gives the single-prediction control law

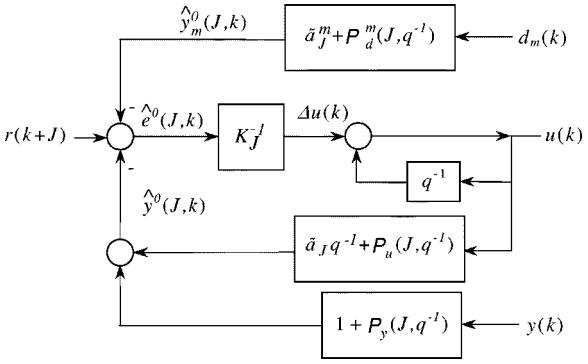

Fig. 2. Structure of the single-prediction controller.

$$u(z)=\{r(J,z)-[1+\mathcal{P}_y(J,z)]y(z) -[\tilde{a}_J^m+\mathcal{P}_d^m(J,z)]d_m(z)\}/[\tilde{a}_J+\mathcal{P}_u(J,z)]. \tag{39}$$

Inspection of this equation revels that the single-predictive controller uses the future reference $[r(k+J)]$. If this one is not available the actual reference $r(k)$ must be used, with the consequential loss of performance during the setpoint tracking. Besides, it also includes a feedforward action introduced by the inclusion of the disturbance prediction $d^0(J,k)$.

Fig. 2 shows a block diagram of how the control action is computed. It is apparent that it uses the plant model to estimate the output at the present time $\hat{y}(k)$. This value is then compared with the actual measurement $y(k)$ to detect modeling errors and external disturbances. Then, the prediction of the disturbance $d^0(J,k)$ is added to estimate $d(J,k)$. In other words, given all the input changes accounted for until the instant k, the single-prediction controller observes the value that would be reached by the system output if no future control action is taken and then $u(k)$ is computed such that the performance index (35) is minimized. Hence, the output reaches the reference value J sampling intervals later.

In this figure we can also see, after some block manipulation, that the single-prediction controller resembles a three degree of freedom structure. However, the controller has only one parameter: namely the *prediction time* J.

4.2. Stability analysis

To analyze the effect of the prediction time on the closed-loop stability, substitute the control law (39) into the closed-loop characteristic equation to obtain

$$T(z)=[\tilde{a}_J+\mathcal{P}_u(J,z)+P_u(0,z)]D(z)+[\mathcal{P}_y(J,z)+P_y(0,z)]N(z). \quad (40)$$

Recalling

$$D(z)=1-P_y(0,z),$$

$$N(z)=P_u(0,z),$$

and combining this expression with Eq. (15), this equation becomes

$$T(z)=[\tilde{a}_J+\tilde{P}_u(J,z)-\tilde{P}_u(0,z)+P_u(0,z)]\times[1-P_y(0,z)]+[\tilde{P}_y(J,z)-\tilde{P}_y(0,z)+P_y(0,z)]P_u(0,z),$$

or simply

$$T(z)=[\tilde{a}_J+\tilde{P}_u(J,z)-\tilde{P}_u(0,z)+P_u(0,z)]+\frac{P_u(0,z)}{1-P_y(0,z)}[\tilde{P}_y(J,z)-\tilde{P}_y(0,z)+P_y(0,z)]. \quad (41)$$

Combining this expression with the expression of $P_y(J,z)$ and $P_u(J,z)$ [Eqs. (10)] we obtain the characteristic equation of closed-loop system,

$$T(z)=\tilde{a}_J+\sum_{j=1}^{p}\tilde{\beta}_j^J z^{-j}+\sum_{j=0}^{p}(\beta_j-\tilde{\beta}_j)z^{-j}+\frac{\Sigma_{i=0}^{p}\beta_i z^{-i}}{1-\Sigma_{i=1}^{p}\alpha_i z^{-i}}\times\left[\sum_{j=1}^{p}\tilde{\alpha}_j^J z^{-j}+\sum_{j=1}^{p}(\alpha_j-\tilde{\alpha}_j)z^{-j}\right]. \quad (42)$$

Theorem 1: Given a system controlled by the control law (39), the closed-loop system will be robustly stable if

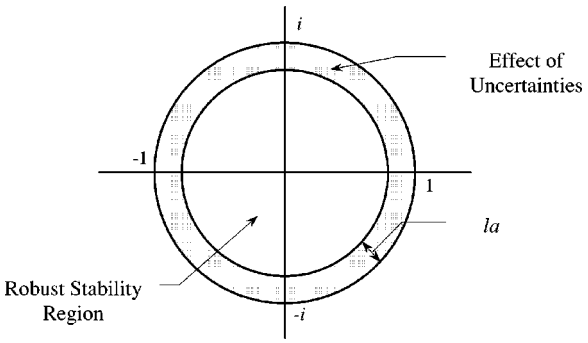

Fig. 3. Geometric interpretation of Eq. (4.11).

$$\tilde{a}_J>\sum_{j=1}^{p}|\beta_j^J|+|K|\sum_{j=1}^{p}|\alpha_j^J|+\sum_{j=0}^{p}|\beta_j-\tilde{\beta}_j|+|K|\sum_{j=1}^{p}|\alpha_j-\tilde{\alpha}_j|, \quad (43)$$

where K is the process gain.

Proof: See Appendix B.

The terms involved in this condition, ordered from left to right, are (a) the contribution of the nominal model, and (b) the effect of parametric uncertainty. From the geometrical point of view, this condition can be visualized as a reduction of the stability region in a size of la (see Fig. 3),

$$la=\sum_{j=0}^{p}|\beta_j-\tilde{\beta}_j|+|K|\sum_{j=1}^{p}|\alpha_j-\tilde{\alpha}_j|.$$

This means that the robust stability region is defined by the circle of radius $1-la$, so the stability condition (43) guarantees that all of poles of the closed-loop system are inside of this region. When there is not uncertainty in the system, Eq. (43) becomes

$$\tilde{a}_J>\sum_{j=1}^{p}|\beta_j^J|+|K|\sum_{j=1}^{p}|\alpha_j^J|, \quad (44)$$

and the *robust stability region* is the unit circle.

Generally, control engineers assume that a family $\mathcal{W}$ of M linear models is able to capture a moderate nonlinearity. Therefore, to guarantee the stability of the system we must choose a J such that it guarantees the stability of all the plants of $\mathcal{W}$. Then, the robust stability problem becomes the problem of finding a J such that Eq. (43) is satisfied for each model of $\mathcal{W}$. Using parametric uncertainty Eq. (43) becomes

$$\tilde{a}_J > \sum_{j=1}^{p} |\beta_j^J| + |K| \sum_{j=1}^{p} |\alpha_j^J| + \max_{l \in [1,M]} \left\{ \sum_{j=0}^{p} |\beta_j^l - \tilde{\beta}_j| + |K^l| \sum_{j=1}^{p} |\alpha_j^l - \tilde{\alpha}_j| \right\}. \tag{45}$$

This means it is necessary to guarantee the stability of closed-loop for the worst case model, compared with the nominal model. From the geometrical point of view means that we choose the bigger uncertainty ($\overline{la}$),

$$\overline{la} = \max_{l \in [1,M]} la^l = \max_{l \in [1,M]} \left\{ \sum_{j=0}^{p} |\beta_j^l - \tilde{\beta}_j| + |K^l| \sum_{j=1}^{p} |\alpha_j^l - \tilde{\alpha}_j| \right\},$$

and the robust stability region is the smallest.

Another way to solve the robust stability problem is to find a J that satisfies simultaneously Eq. (44) for all the models of $\mathcal{W}$. In case of a system with monotone response, the stability condition (45) can be written as

$$J_{\mathrm{STB}} = \max(J_1; J_2; \ldots; J_M), \tag{46}$$

where J_l $l = 1,2,\ldots,M$ is the prediction time for the lth model of the family $\mathcal{W}$. This expression means that we can chose a different prediction time for each model of $\mathcal{W}$, then we selected the bigger prediction time.

A final remark is for recalling that the stability condition given by Dabke [11] is a sufficient one. Consequently stability conditions (43)–(45) become conservative and impose a too high lower bound for selecting J. So, always there are prediction times lower than J_{STB} for which the closed-loop system will be stable. The first J that guarantees the closed-loop stability can be found through a direct search, because the solution space is bounded

$$1 \leqslant J \leqslant N.$$

Furthermore, the open-loop predictor can be directly built from the nonlinear model, since J_{STB} guarantees the closed-loop stability for all the models of $\mathcal{W}$. The nonlinear predictor can be built from the nonlinear model employing a numerical integration scheme or using a local model network [12].

5. Predictive feedback control

5.1. The control algorithm

Giovanini [4] has established that the single-prediction controller provides a similar closed-loop performance to a MPC controller with fixed parameters. This fact means that a single-prediction controller has a poor closed-loop performance when there are disturbances and/or uncertainties in the system. Thus, he introduced a direct feedback mode in the computation of the control action through the inclusion of a filter into the single-prediction control law (38). Since it employs only one prediction of the process future behavior, he applied the delay operator q^{-i}, $i = 0,1,\ldots,w$, to the time instant at which the prediction is calculated. Hence, the control change $\Delta u(k)$ is given by

$$\Delta u(k) = \sum_{i=0}^{w} \delta_i \hat{e}^0(J, k-i), \tag{47}$$

where $\hat{e}^0(J,k-i)$ is the J-step ahead open-loop error computed at time $k-i$, $w \in Z$ is the filter order, and δ_i $i \in [0,w]$ are the controller parameters. The predictive feedback control law can be derived from Eq. (47), replacing the open-loop error $\hat{e}^0(J,k-i)$ by their components and following a similar procedure to obtain Eq. (39). The result is

$$u(z) = \frac{F(z)r(z) - F(z)[1 + \mathcal{P}_y(J,z)]y(z)}{(1-z^{-1})\tilde{a}_J + F(z)[\tilde{a}_J z^{-1} + \mathcal{P}_u(J,z)]} - \frac{F(z)[\tilde{a}_J^m z^{-1} + \mathcal{P}_d^m(J,z)]d_m(z)}{(1-z^{-1})\tilde{a}_J + F(z)[\tilde{a}_J z^{-1} + \mathcal{P}_u(J,z)]}, \tag{48}$$

whose structure is shown in Fig. 4. Giovanini [4] pointed out that $F(z)$ adds additional degrees of freedom to improve the closed-loop performance and makes the controller tuning difficult. However, he showed that the prediction time (J) and the parameters of the filter (w and δ_i $i \in [0,w]$) can be independently fixed to each other (see Appendix B). So, the prediction time will be chosen

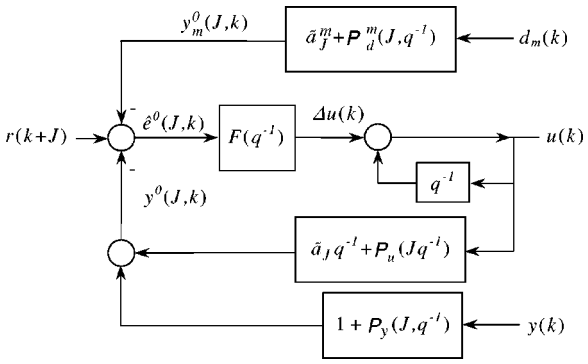

Fig. 4. Structure of the predictive feedback controller.

based on stability criteria for the single-prediction controller [Eqs. (44)–(46)] and, then the filter parameters will be fixed using a tuning method for fixed-structure controller [13].

This new formulation of predictive control combines the capacity of the predictive algorithm and the classical use of feedback information with the capabilities of estimation techniques. So, it provides a better performance than the original formulation of this controller (as we can see in the examples) and a linear MPC controller [4]. Also note that the predictive feedback controller, in both formulations, has two degrees of freedom: the prediction time J and the filter $F(z)$.

5.2. Stability analysis

Now, we study the effect of the filters and prediction time on the closed-loop stability. First, we substitute the predictive feedback controller (48) in the characteristic closed-loop equation, which becomes

$$T(z)=D(z)\{(1-z^{-1})\tilde{a}_J+F(z)[\tilde{a}_J z^{-1}+\mathcal{P}_u(J,z)+P_u(0,z)]\}+N(z)F(z)[\mathcal{P}_y(J,z)+P_y(0,z)]. \quad (49)$$

Combining this expression with Eq. (15), the characteristic equation $T(z^{-1})$ can be written as follows:

$$T(z)=\{(1-z^{-1})\tilde{a}_J+F(z)\tilde{a}_J z^{-1}+F(z)[\tilde{P}_u(J,z)-\tilde{P}_u(0,z)+P_u(0,z)]\}[1-P_y(0,z)]+P_u(0,z)F(z)[\tilde{P}_y(J,z)-\tilde{P}_y(0,z)+P_y(0,z)].$$

The stability of the closed-loop system depends on both the prediction time J and the parameters of the filter $F(z)$. So, it may be tested by any usual stability criteria.

Theorem 2: Given a system controlled by the control law (48), the closed-loop system will be robustly stable if

$$\tilde{a}_J > \sum_{j=1}^{p} |\tilde{\beta}_j^J| + |K| \sum_{j=1}^{p} |\tilde{\alpha}_j^J| + \sum_{j=0}^{p} |\beta_j - \tilde{\beta}_j| + |K| \sum_{j=1}^{p} |\alpha_j - \tilde{\alpha}_j|. \quad (50)$$

Proof: See Appendix B

This stability condition is the same stability condition for the single-prediction controller [Eq. (43)]. This result was previously obtained by Giovanini [4]. It means that the prediction time J and the parameters of the filter can be independently selected such that both parameters, J and δ_i $i \in [0,w]$, independently guarantee the closed-loop stability. This fact means that the prediction time J should be selected like the single-prediction controller [Eqs. (43)–(46)], and the filter must be tuning as there is no time delay in the system, because it has been compensated by the open-loop predictor.

Remark 1: Since the prediction time J can be fixed independently of the filters, parameters may be tuned so that the closed-loop performance is improved. Varying J the closed-loop settling time can be modified, accelerating or decelerating the system response. So, if we have to control a nonlinear system we can choose a different J for each operating region such that we obtain a similar closed-loop response for each one of them. Then, during the operation, we vary J according to the operating region controlled at each sample.

6. Simulations

In this section two simulation examples are considered to show the effectiveness of the controllers

proposed in this work. In the first example we consider the model of a distillation column previously used by Prett and Morari [14] for evaluating linear control strategies. In this example we compare two classical (feedback and cascade) control strategies and the original formulation of single-prediction control [4] with the new one for disturbance rejection. In the second example we consider a continuous stirred tank reactor, which was previously used by several authors [15,16] to test discrete control algorithms. In this example we compare the responses obtained by predictive feedback controllers, the original formulation and that one proposed in this work, and a PI for tracking setpoint and rejecting disturbances.

Example 1: Prett and Morari [14] have provided a distillation column case study for evaluating control strategies. We use a subset of the problem to illustrate and evaluate the ideas presented above. The process model is

$$y(s)=4.05\frac{e^{-27s}}{50s+1}u(s)+1.44\frac{e^{-27s}}{40s+1}d(s), \tag{51a}$$

$$t(s)=3.66\frac{e^{-2s}}{9s+1}u(s)+1.27\frac{1}{6s+1}d(s). \tag{51b}$$

Note that the secondary variable $t(s)$ responds much faster to both variables, manipulated and disturbance, than the primary variable $y(s)$. For direct feedback control $y(s)$, the tuning constant for the PID *controller is obtained by applying* IMC *tuning rules to the transfer function between $y(s)$ and $u(s)$ with the filter time constant $\tau_f=10$. Two controllers must be designed for the cascade control scheme. For the inner loop, the transfer function between $t(s)$ and $u(s)$ is used to get the tuning constants with $\tau_f=2$. The outer loop controller is designed from the model obtained for the inner loop, which was obtained from a step response experiment. This model is used to design a PID using IMC rules with $\tau_f=10$. The controller tuning constants for all these schemes are shown in Table I.*

To develop both predictive controllers, the system (51) is discretized with a sampling time of 1 s. The single-predictive controller without estimator was directly developed from the discretized model. The single-prediction controller with estimator was developed from the estimators building from the space-state model of Eq. (51) assuming a deadbeat behavior since there are no uncertainties.

Then, the open-loop predictors for the system output was developed from these models employing Eqs. (15) and (32). The prediction time for both predictive controllers were chosen using the stability condition (44), so J must satisfy

$$J\geqslant 38.$$

Since it is known that Dabke's condition is conservative, we explore the solution space and find that the prediction time that provides the better performance is

$$J=30.$$

Fig. 5 shows the responses of the controllers using the control schemes designed above to reject a load disturbance change. The excellent disturbance rejection capabilities of the predictive control with embedded estimator is seen clearly in these graphs. Note that because the longer time constant and large time delay in the outer loop of the cascade scheme, this controller cannot be expected to respond quickly to the input disturbance.

Table 1
Tuning constants used in the classical control schemes.

Control schemes	Tuning constants
Direct feedback on y	$Kc=2.12$, $\tau_I=50$, $\tau_D=13.5$
Cascade control (outer loop)	$Kc=0.2$, $\tau_I=50$, $\tau_D=10$
Cascade control (inner loop)	$Kc=0.81$, $\tau_I=9$

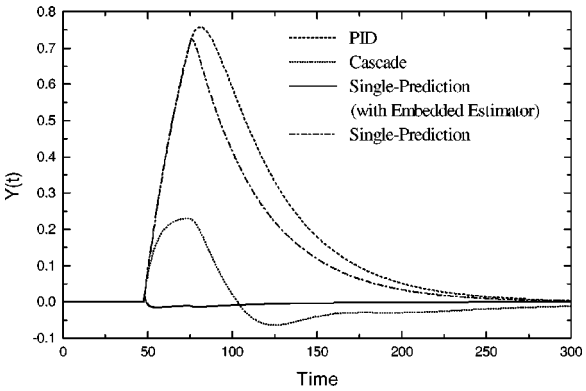

Fig. 5. Closed-loop responses of the linear system to a step change in disturbance for different control schemes.

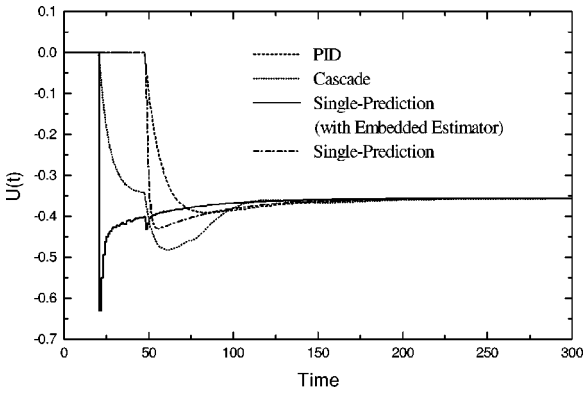

Fig. 6. Control variable correspondent to the closed-loop responses shown in Fig. 5.

Fig. 6 shows the control actions employ by each control scheme to reject the disturbance. It is easy to see the feedforward action introduced by the estimator. The control action is applied to the system as soon as the disturbance is detected in any output of the system.

Example 2: Now, let us consider the problem of controlling a continuous stirred tank reactor (CSTR) *in which an irreversible exothermic reaction is carried out at constant volume. This is a nonlinear system originally used by Morningred et al. [16] and Giovanini [4] for testing predictive control algorithms. The objective is controlling the output concentration* $Ca(t)$ *using the coolant flow rate* $q_C(t)$ *as the manipulated variable. The disturbances considered in this work are the inlet coolant temperature* $T_{CO}(t)$ *(measurable) and the feed concentration* $Ca_O(t)$ *(nonmeasurable). The output concentration has a measured time delay of* $t_d = 0.5$ min.

The nonlinear nature of the system is shown in Figs. 7 and 8, where we can see the open-loop response to changes in the manipulated and the disturbances. Fig. 7 shows the dynamic responses to the following sequence of changes in the manipulated variable $q_C(t)$: $+10$, -10, -10, *and* $+10\ \mathrm{lt\,min^{-1}}$. *Fig. 8 shows the dynamic responses to changes in the disturbances variables, first changes in the inlet concentration* $Ca_O(t)$ ($+0.05$ *and* -0.05 mol $\mathrm{lt^{-1}}$) *and later in the refrigerant temperature* $T_{CO}(t)$ ($+10$ and $-10\,^{\circ}C$).

From these figures it is easy to see that the reactor is quite difficult to control due to the change in the dynamic from one operational condition to another and the presence of zeros near imaginary axis. These facts are especially important for disturbances rejection problem. So, to obtain a good performance an important control energy will be required. Besides, the CSTR *becomes uncontrollable when* $q_C(t)$ *go to beyond of* $113\ \mathrm{lt\,min^{-1}}$.

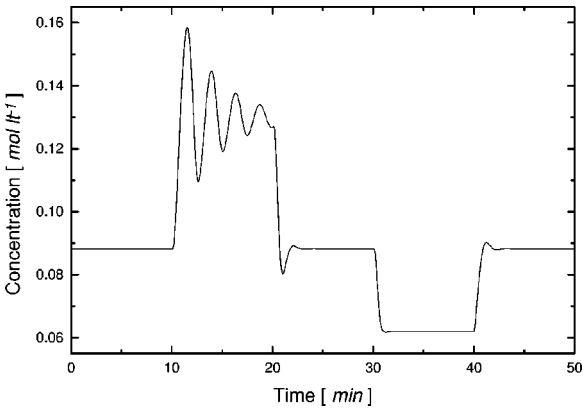

Fig. 7. Open-loop response to change in $q_C(t)$.

We are interested in controlling the reactor around the nominal operating region. So we develop the controllers from the linear model that resulting from the linearization of the reactor at nominal parameters and $q_C = 100\ \mathrm{lt\,min^{-1}}$. *The linear model is*

$$\begin{bmatrix} \dot{Ca}(t) \\ \dot{T}(t) \end{bmatrix} = \begin{bmatrix} -101.3 & 10.1 \\ 25.3 & 0.001 \end{bmatrix} \begin{bmatrix} Ca(t) \\ T(t) \end{bmatrix} + \begin{bmatrix} 0 \\ -0.004 \end{bmatrix} q_C(t) + \begin{bmatrix} 1 & 0 \\ 0 & 0.02 \end{bmatrix} \times \begin{bmatrix} Ca_O(t) \\ T_{CO}(t) \end{bmatrix}, \tag{52}$$

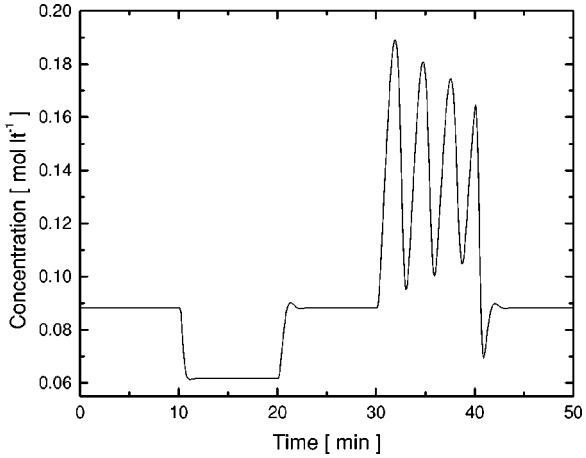

Fig. 8. Open-loop response to changes in $Ca_O(t)$ and $T_{CO}(t)$.

which was discretized assuming a zero-order hold in the input and a sampling time $t_S = 0.1\ seg$.

The controller must be able to follow the reference and reject the disturbances present in this system. Besides, the closed-loop response should satisfy the following constraint:

$$q_C(k) \leqslant 10, \quad \forall k, \tag{53}$$

to guarantee the controllability of the system. This assumes that the nominal absolute value for the manipulated $q_C(k)$ *is around* $100\ \mathrm{lt\,min^{-1}}$ *and that the operation is kept near the nominal conditions. Besides, a zero-offset steady-state response is demanded, then we include the following constraints:*

$$\sum_{j=1}^{v} \phi_j = -1. \tag{54}$$

This assumes that the nominal absolute value for the manipulated is around $100\ \mathrm{lt\,min^{-1}}$ *and that the operation is kept inside the polytope whose vertices are defined by the linear models. The constraints (53) and (54) are then included in the tuning problem.*

To develop the predictive feedback controller with embedded estimator, estimators for Ca *and* Ca_O *must first be developed from the discrete model of Eq. (52) assuming a deadbeat behavior. Then, the open-loop predictors for* Ca *were developed from these estimators and the discretization of model (52) using Eqs. (10), (31), and (32). Since an integral action is demanded, the prediction time J was chosen using the stability condition (44). Therefore, the prediction time was fixed*

$$J = 9.$$

Finally, the order of the filter was chosen such that the resulting controllers include the predictive version of popular PID $(w = 2)$.

In a first step we consider the predictive feedback controller with embedded estimator. The parameters of the filters were fixed by solving the tuning problem proposed by Giovanini and Marchetti [15] for step changes in all inputs, the objective function:

$$L = \sum_{k=1}^{N} e^2(k) + \lambda \Delta u^2(k), \tag{55}$$

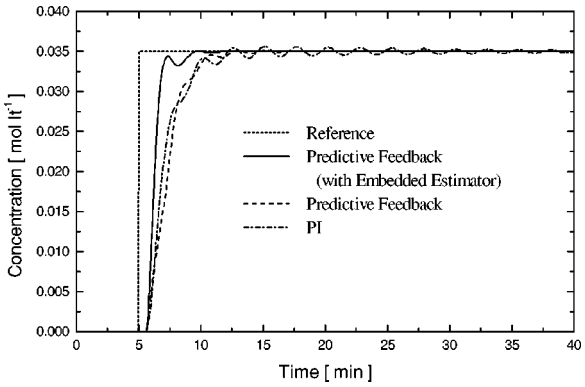

Fig. 9. Closed-loop responses of the linear system due to a step change in setpoint.

and the design constraints (53) and (54). The control weight was fixed in a value such that the control energy has a similar effect than errors in the tuning process $(\lambda = 0.01)$. *The behavior of the closed-loop system evaluated over* $N = 300$ *sampling instants. The problem described to this point has a fast solution using an algorithm based on descendent gradient method. The filter parameters of the filter are*

$$\delta_0 = 0.7655, \quad \delta_1 = -0.1251, \quad \delta_2 = -0.495. \tag{56}$$

To evaluate the effects of estimators on the closed-loop performance we compare the responses obtained by a predictive feedback controller with the same parameters, the same objective function and design constraints as the previous predictive controller. The only difference is the predictor, which was directly developed from the discrete model of Eq. (52) and includes the inlet coolant temperature $T_{CO}(t)$ *to improve the closed-loop performance. Solving again the previous tuning problem we obtain the following parameters*:

$$\delta_0 = 0.6883, \quad \delta_1 = -0.071, \quad \delta_2 = -0.395. \tag{57}$$

Morningred et al. [16] have previously worked with this model for testing predictive controllers and they compared their results with the responses obtained using a PI *controller, whose parameters were adjusted by* ITAE *criterion. Thus, we used the same settings*

$$Kc = 52, \quad \tau_I = 0.46.$$

Fig. 9 shows the results obtained when comparing

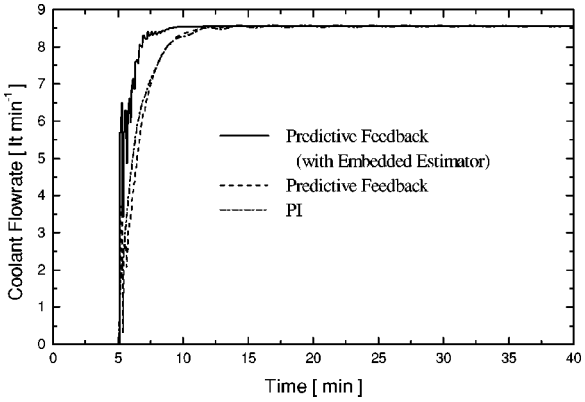

Fig. 10. Control variable corresponding to the closed-loop responses shown in Fig. 9.

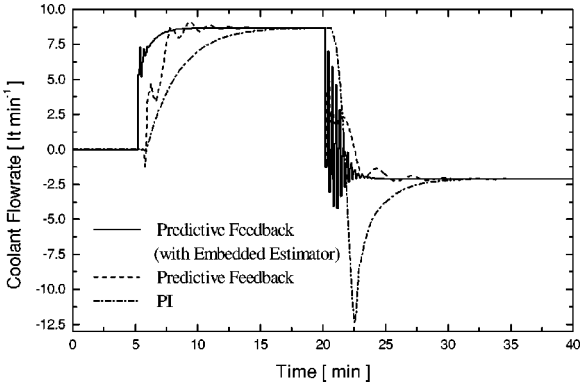

Fig. 12. Control variable corresponding to the closed-loop responses shown in Fig. 11.

the responses obtained for a set point change. The superior performance of the proposed control scheme is obtained through the better use of information available in the system. This fact is shown by the movement in the manipulated variable, which does not overcome the upper bound $[q_C(k) \leqslant 10 \ \forall k]$ *limit as shown in Fig. 10, but shows more movements than the other controllers. This fact happens due to the open-loop dynamic of the reactor. In fact, in Fig. 9 we can also see that the response of the* PI *exhibits the oscillatory behavior of the system (see Fig. 7).*

Fig. 11 shown the results obtained when comparing both predictive controllers under load changes. For testing the disturbance rejection the following sequence of changes is made: first the feed stream concentration $Ca_O(t)$ *goes down* $0.05 \ \mathrm{mol\,lt^{-1}}$ *and* 15 *min later the refrigerant temperature* $T_{CO}(t)$ *goes down* $10\,^{\circ}\mathrm{C}$. *A better disturbance rejection capability is observed in the discrete controller suggested in this paper.*

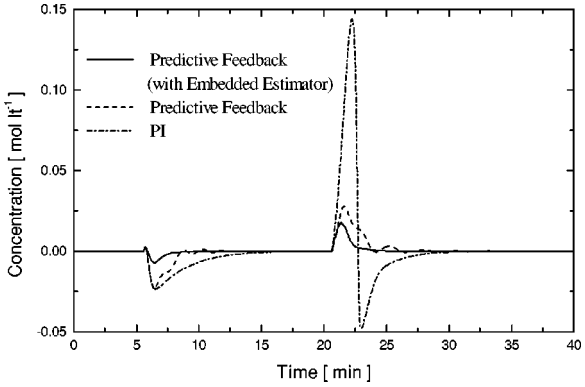

Fig. 11. Closed-loop responses of the linear system to a step change in $Ca_O(t)$ and $T_{CO}(t)$.

In Fig. 12 we see the same problem with the manipulated variable, but increased. The excursion of q_C *is more important in the case of* PI, *but smoother. The predictive feedback controller employs more energy to control the system due to feedforward action introduced by the estimator. We can solve the problem increasing the control weight* λ *in the objective function (55) or varying the closed-loop settling time through a greater prediction time J (the last option is easier to implement because we do not need to retune the parameters of the controller). These facts have the same effect: reduce the control energy by degrading the closed-loop performance.*

7. Conclusions

A new alternative method for designing a predictor from the ARMAX model was presented. The resulting predictor employs the implicit observer information embedded in the input-output model and retains the key benefits of the space-state approach to improve the prediction of the system output. Then, it was used to develop a predictive feedback controller. The new formulation of a predictive controller includes feedback and feedforward actions that improve the closed-loop performance, especially when unmeasured disturbances and time delay are present in the system.

Closed-loop responses were obtained to show the successful working of this framework in rejecting nonmeasurable disturbances and compensating time delay. Two case studies of the shell

challenge problem were used to highlight the advantages of the control scheme compared to conventional control strategies.

Acknowledgment

The author is grateful for the financial support for this work provided by the Engineering and Physical Science Research Council (EPSRC) grant Industrial Non-linear Control and Applications GR/R04683/01.

Appendix A: Proof of Lemma 2.1

Employing the state space model (4), the J step ahead prediction is given by

$$\hat{y}(J,k)=Cx(k+J)+Du(k+J). \tag{A1}$$

Assuming that the state $x(k)$ is measurable, the output prediction is given by

$$\hat{y}(J,k)=CA^{J}x(k)+\sum_{j=0}^{J-1} CA^{j}Bu(k+J-j) + Du(k+J)+\sum_{j=0}^{J-1} CA^{j}B_d d_m(k+J-j). \tag{A2}$$

Comparing this equation with Eq. (8), we can see that the effect of the effect of the future inputs is given by

$$\tilde{\beta}_0^j=CA^jB \quad j=1,2,\ldots,J,$$
$$\tilde{\beta}_0^0=D, \tag{A3}$$

and

$$\tilde{\gamma}_0^j=CA^jB_d \quad j=1,2,\ldots,J. \tag{A4}$$

which are the jth coefficient of the impulse response of G_p and G_d, respectively.

If the state $x(k)$ is not measurable, it can be estimated using an observer

$$x(k)=\mathcal{A}^k x(0)+\sum_{j=0}^{k-1} C\mathcal{A}^j Bu(k-j) + \sum_{j=0}^{k-1} C\mathcal{A}^j B_d d_m(k-j) + \sum_{j=0}^{k-1} C\mathcal{A}^j y(k-j),$$

where $\mathcal{A}=A-KC$. Assuming that k is large enough to dismiss its contribution we obtain

$$\hat{y}(J,k)=\sum_{j=0}^{k-1} C\mathcal{A}^{J+j}Bu(k-j) + \sum_{j=0}^{k-1} C\mathcal{A}^{J+j}B_d d_m(k-j) + \sum_{j=0}^{k-1} C\mathcal{A}^{J+j}Ky(k-j) + \sum_{j=0}^{J-1} C\mathcal{A}^{j}Bu(k+J-j)+Du(k+J) + \sum_{j=0}^{J-1} C\mathcal{A}^{j}B_d d_m(k+J-j).$$

Comparing this equation with Eq. (8), we can see that the effect of the past inputs on the future output is stated by

$$\mathcal{P}_u(J,z)=\sum_{j=0}^{k-1} C\mathcal{A}^{J+j}B=\sum_{j=J+1}^{N} \tilde{h}_j q^{-j}, \tag{A5}$$

$$\mathcal{P}_d^m(J,z)=\sum_{j=0}^{k-1} C\mathcal{A}^{J+j}B_d=\sum_{j=J}^{N} \tilde{h}_j^d q^{-j}, \tag{A6}$$

which are the open-loop predictors defined in previous work by Giovanini [4].

Appendix B: Stability criteria for predictive feedback control

The characteristic closed-loop equation $T(z)$ for the predictive feedback control (48) is given by

$$T(z)=D(z)\{(1-z^{-1})\tilde{a}_J+F(z)[\tilde{a}_J z^{-1}+\mathcal{P}_u(J,z) + P_u(0,z)]\}+N(z)F(z)[\mathcal{P}_y(J,z) + P_y(0,z)].$$

Recalling

$$D(z)=1-P_y(0,z),$$
$$N(z)=P_u(0,z),$$

and combining this expression with Eq. (15), the characteristic equation becomes

$$T(z)=\{(1-z^{-1})\tilde{a}_J+F(z)\tilde{a}_J z^{-1}+F(z)[\tilde{P}_u(J,z)-\tilde{P}_u(0,z)+P_u(0,z)]\}[1-P_y(0,z)]+P_u(0,z)F(z)[\tilde{P}_y(J,z)-\tilde{P}_y(0,z)+P_y(0,z)],$$

or simply

$$T(z)=(1-z^{-1})\tilde{a}_J+F(z)\tilde{a}_J z^{-1}+F(z)\times\left\{\tilde{P}_u(J,z^{-1})+\frac{P_u(0,z)}{1-P_y(0,z)}\tilde{P}_y(J,z)\right\}+F(z)\left\{[P_u(0,z)-\tilde{P}_u(0,z)]+\frac{P_u(0,z)}{1-P_y(0,z)}[P_y(0,z)-\tilde{P}_y(0,z)]\right\}.$$

The stability of the closed-loop system depends on the prediction time J and may be tested by any usual stability criteria. First, the following lemma is introduced.

Lemma 3: If the polynomial $T(z)=1+\sum_{i=0}^{p}h_i z^{-i}$ *has the property that*

$$\inf_{|z|\geq 1}|T(z)|<0,$$

then the related closed-loop system will be asymtoptically stable [11].

Hence,

$$|T(z)|\geq|(1-z^{-1})\tilde{a}_J|+|F(z)||\tilde{a}_J z^{-1}|-|F(z)|\left\{|\tilde{P}_u(J,z)|+\left|\frac{P_u(0,z)}{1-P_y(0,z)}\right||\tilde{P}_y(J,z)|\right\}-|F(z)|\left\{|P_u(0,z)-\tilde{P}_u(0,z)|+\left|\frac{P_u(0,z)}{1-P_y(0,z)}\right||P_y(0,z)-\tilde{P}_y(0,z)|\right\}$$

and again using Lemma 1 gives

$$\tilde{a}_J>|\tilde{P}_u(J,1)|+|K||\tilde{P}_y(J,1)|+|P_u(0,1)-\tilde{P}_u(0,1)|+|K||P_y(0,1)-\tilde{P}_y(0,1)|, \tag{B1}$$

where K is the system gain given by

$$K=\frac{\Sigma_{i=0}^{p}\beta_i}{1-\Sigma_{i=1}^{p}\alpha_i}.$$

Finally, combining this expression with the expression of $P_y(J,z)$ and $P_u(J,z)$ [Eqs. (10)] we obtain the characteristic equation of closed-loop system

$$\tilde{a}_J>\sum_{j=1}^{p}|\tilde{\beta}_j^J|+|K|\sum_{j=1}^{p}|\tilde{\alpha}_j^J|+\sum_{j=0}^{p}|\beta_j-\tilde{\beta}_j|+|K|\sum_{j=1}^{p}|\alpha_j-\tilde{\alpha}_j|. \tag{B2}$$

Remark 2: If $F(z)=1$ *the predictive feedback controller becomes the single-prediction and the stability condition for this controller is Eq. (B2).*

References

[1] Clarke, C., Mothadi, D., and Tuffs, P., Generalized predictive control: The basic algorithm. Automatica **24**, 137–160 (1987).

[2] Isermann, R., Digital Control Systems. Springer-Verlag, Berlin, 1998.

[3] Arulalan, G. and Deshpande, P., Simplified model predictive control. Ind. Eng. Chem. Res. **26**, 347–356 (1987).

[4] Giovanini, L., Predictive feedback control. ISA Trans. **42**, 207–226 (2003).

[5] Goodwin, G. and Sin, K., Adaptive Filtering and Prediction and Control. Prentice Hall, Englewood Cliffs, NJ, 1984.

[6] Baras, J., Bernsoussan, A., and James, M., Dynamic observers as asymptotic limits of recursive filters: Special cases. SIAM (Soc. Ind. Appl. Math.) J. Appl. Math. **48**, 1147–1158 (1994).

[7] Gertler, J., Generating directional residuals with dynamic parity relations. Automatica **31**, 627–635 (1995).

[8] Kitanidis, P. K., Unbiased minimum-variance linear state estimation. Automatica **23**, 775–778 (1987).

[9] Keller, J., Fault isolation filter design for linear stochastic systems. Automatica **35**, 1701–1706 (1999).

[10] Wojsznis, W., Variable Horizon Predictor, *Proceedings of the 33rd Conference on Decision and Control*, Lake Buena Vista, Florida, December, 1994.

[11] Dabke, K., A simple criterion for stability of linear discrete systems. Int. J. Control **37**, 657–659 (1983).

[12] Prasad, G., Swidenbank, E., and Hogg, B., A local model network based multivariable long-range predictive control strategy for thermal power plants. Automatica **34**, 1185–1204 (1998).
[13] Abbas, A. and Sawyer, P., A multiobjective design algorithm: Application to the design of SISO control systems. Comput. Chem. Eng. **19**, 241–248 (1995).
[14] Prett, D. and Morari, M., *The Shell Process Control Workshop* **47**, 755–765, Butterworths, Stoneham, MA, 1986.
[15] Giovanini, L. and Marchetti, J., Shaping time-domain response with discrete controllers. Ind. Eng. Chem. Res. **38**, 4777–4789 (1999).
[16] Morningred, J., Paden, B., Seborg, D., and Mellichamp, D., An adaptive nonlinear predictive controller. Chem. Eng. Sci. **47**, 755–765 (1992).

Leonardo L. Giovanini was born in Argentina in 1969. He received the B.SC. (Honors) degree in Electronic Engineering form the Universidad Tecnologica Nacional, Regional School at Villa Maria in 1995, and the Ph.D. degree in Engineering Science from Universidad Nacional del Litoral, School of Water Resource in 2000. Since then he has been Lecturer in the Department of Electronic Engineering at Universidad Tecnologica Nacional, Regional School at Villa Maria. Actually, he is working as a research fellow in the Industrial Control Center, University of Strathclyde. His research interests include predictive control for non-linear systems, fault detection and isolation, fault tolerant control, and distributed control systems.